



## Gradual Change of Pulse Parameters as a New Strategy for Synthesis of Functionally Graded Ni-Cr Coatings

Touraj Abedi<sup>1</sup>, Shahin Khameneh Asl<sup>\*1</sup>, Mohamadreza Etminanfar<sup>2</sup>

<sup>1</sup>Department of materials engineering, Faculty of Mechanical Engineering, university of Tabriz, Tabriz, Iran.

<sup>2</sup>Faculty of Materials Engineering, Sahand University of Technology, Tabriz, Iran.

Received: 02 March 2019; Accepted: 05 May 2019

\* Corresponding author email: [khameneh@tabrizu.ac.ir](mailto:khameneh@tabrizu.ac.ir)

### ABSTRACT

Synthesis of functionally gradient coating was the main goal of researches to cover some deficiencies of metallic coatings. In this study, a new strategy for generating functionally gradient coatings of nickel-chromium on a carbon steel substrate using pulse electrodeposition has been presented. The gradual changes of the duty cycle and pulse frequency were used to generate the functionally gradient coating, and the chemical composition, microstructure, microhardness, wear and corrosion of them were investigated. Gradual changes of the duty cycle from 45 to 80% led to a gradient structure with a chromium content of 83% on the surface and 3% in the vicinity of the interface. Frequency changes had no significant effect on the chemical composition and did not result in the production of gradient coatings. In both groups, wear resistance improved related to the monolayer one so that weight loss in former group is reduced about 33-62% and in later group decreased almost 13-30%. Also, the corrosion current density in the samples deposited by gradual change of duty cycle was approximately 0.01-0.04 times of that for monolayer coatings. The microhardness value in the top layers of FGD coating was in the range of 650-800 HV<sub>0.01</sub> which reduced gradually towards the substrate. The high Cr content in the top layers is the reason for high hardness and good corrosion resistance.

**Keywords:** Electrodeposition; Functionally graded coating; Duty cycle; Frequency.

### 1. Introduction

The use of Cr coatings is very wide-spread for industrial parts to confront corrosion and wear damages [1]. On the other hand, the use of hexavalent Cr bath due to environmental problems and human hazards is very limited and is prohibited in many parts of the world [2]. Therefore, the use of trivalent Cr is very much considered. Trivalent Cr has lower hardness and corrosion resistance than hard chromium [3]. Various ideas have been used to solve this problem; alloying with other metals as well as creating a multilayer structure. In the field of

Cr alloy coating, alloying with iron group metals is very common, which has somewhat improved the properties of coatings [4]. The idea of multilayer coatings has been used in many different systems and in various ways. For instance, Huang and Etminanfar [5] electrodeposited Ni-Cr multilayer coatings in which the Cr-rich and Ni-rich layers are deposited decussate. In these coatings multilayered structure improved the corrosion resistance. The use of laminar structure has also been used to increase the hardness, strength and corrosion resistance of Ni-Fe and Ni-Fe-Cr coatings [6-9]. One of the

most important features of the layered structure is to prevent the interconnection of defects and micro-cracks [10]. Since there are many fine and coarse cracks in Cr coatings, due to the formation of chromium hydrates during the deposition and release of hydrogen afterward, a layered structure with a lower Cr content between the Cr-rich layers can prevent crack propagation, and thus has a major contribution to increasing corrosion resistance [5]. One of the proper methods to create a layered structure and to further improve Cr coatings is to use a chemically gradient structure. This structure is synthesized using a pulsed current electrodeposition method with gradual changes in pulse conditions which is used for Ni-W and Ni-Fe systems [10, 11]. In this way, the pulse duty cycle is gradually changed from low to high or vice versa. The continuous changes of pulse parameters resulted in different compositions in alternative layers as the content of the alloying elements (e.g. W or Fe) gradually altered in cross section [4]. So far, no information has been reported on the Ni-Cr functionally gradient (FG) coating. Deposition of a Cr-poor layer on the substrate for the slightest defects and cracks and the layers with the high Cr content in the outer layers for better corrosion resistance is very interesting and may further extend the use of this method.

There are limited studies about the pulse parameters on characteristics of Ni-Cr. Moreover, corrosion properties and tribological behavior of monolayer and FG Ni-Cr coating have not been comprehensively studied. The main objective of this study is to investigate the effect of pulse parameters on the properties of the monolayer and FG Ni-Cr coatings from a trivalent Cr bath.

## 2. Experimental procedure

### 2.1. Materials and electrodeposition

An AISI 1010 steel was selected as a substrate of electroplating. The steel sheets were cut to proper

pieces of 80×20×1 mm<sup>3</sup> and then abraded by emery papers to obtain the surface roughness of lower than 0.4 μm. The polished samples after cleaning with water were, ultrasonically degreased in acetone and pickled in 20%Vol. HCl solution for 30s. Finally the samples immediately were transferred to the electrodeposition bath. The composition of electrodeposition bath was according to Table 1. distilled water and analytical grades of Merck chemicals were used. The volume of the bath was 200ml and the anode was Pt with a surface area same as the substrate. The pH of the electrolyte was adjusted to 2 and regulated during the deposition process by adding H<sub>2</sub>SO<sub>4</sub> or NaOH solution. The electrolyte was stirred mechanically with a rotating speed of 100 rpm and the temperature was constant at 30°C during the process.

### 2.2. Electrodeposition parameters

In this work at first stage, some monolayer coatings were deposited. The square-shaped pulses were used for all coatings. The pulse duty cycle was in the range of 30-80% and pulse frequency was constant at 25, 100, and 200Hz. The peak current density (*i<sub>p</sub>*) of experiments was constant at 40 A/dm<sup>2</sup> and the average current density (*i<sub>avg</sub>*) was variable. The adjusted parameters are shown in Table 2.

At the second stage, the gradient coatings were deposited. The schematic of deposited coatings is shown in Fig. 1. As exhibited, the consecutive layers deposited in a manner that duty cycle is increased in 7 steps from 45 to 80% at a constant frequency which is named as functionally graded by duty cycle (FGD). In the second category, frequency is increased in 7 steps from 25 to 200Hz at a constant duty cycle which is named as functionally graded by frequency (FGF). The arrangement of layers is regulated according to the information of monolayer coatings. The time of electrodeposition adjusted for a layer thickness of 5μm in FG coatings. The pulse parameters are shown in Table 3.

Table 1- The chemical composition of electrodeposition bath

Cr <sub>2</sub> (SO <sub>4</sub> ) <sub>3</sub> .6H <sub>2</sub> O	100 (g/l)
NiSO <sub>4</sub> .7H <sub>2</sub> O	40 (g/l)
HCOOH	32 (ml/l)
H <sub>3</sub> BO <sub>3</sub>	56 (g/l)
Na <sub>2</sub> SO <sub>4</sub>	71 (g/l)
SDS	0.1 (g/l)

2.3. Evaluations

The microstructure and morphology of electrodeposited specimens were studied by TESCAN-VEGA scanning electron microscope (SEM) and the chemical composition was measured

by energy dispersive spectroscopy (EDS) attached to the SEM device. The Vickers microhardness on the cross section of coatings was performed using 10g load for 15s by SCTMC HV 1000Z microhardness tester. The average of five readings was reported

Table 2- The adjusted parameters for monolayer coatings

Duty cycle (%)	$i_p$ (Adm <sup>-2</sup> )	f (Hz)	t (min) for 15 $\mu$ m
30	40	25, 100, 200	123
40	40	25, 100, 200	107
50	40	25, 100, 200	67.5
60	40	25, 100, 200	51
70	40	25, 100, 200	33
80	40	25, 100, 200	18

Table 3- The regulated pulse parameters for FG coatings

Sample	Pulse parameters		Average current density ( $i_{avg}$ )(Adm <sup>-2</sup> )
	Constant	Changing	
	f (Hz)	Duty cycle (%)	
FGD	25	45-50-55-60-65-70-75-80	18-20-22-24-26-28-30-32
FGD	50	45-50-55-60-65-70-75-80	18-20-22-24-26-28-30-32
FGD	100	45-50-55-60-65-70-75-80	18-20-22-24-26-28-30-32
FGD	150	45-50-55-60-65-70-75-80	18-20-22-24-26-28-30-32
FGD	200	45-50-55-60-65-70-75-80	18-20-22-24-26-28-30-32
	Duty cycle (%)	f (Hz)	
FGF	40	25-50-75-100-125-150-175-200	16
FGF	50	25-50-75-100-125-150-175-200	20
FGF	60	25-50-75-100-125-150-175-200	24
FGF	70	25-50-75-100-125-150-175-200	28
FGF	80	25-50-75-100-125-150-175-200	32

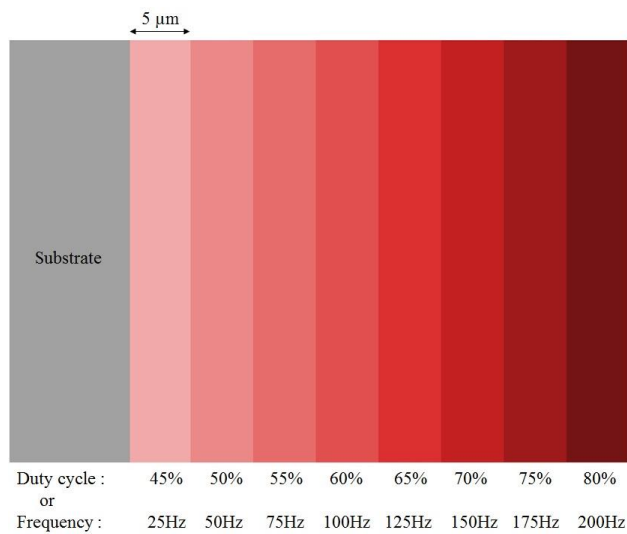


Fig. 1- The schematic of deposited FG coatings.

for each data. The corrosion resistance of different specimens was surveyed by potentiodynamic test using a three-electrode system by AUTOLAB PGSTA T30 in 3.5% NaCl solution at a scan rate of 1mV/s. The coated specimens, platinum, and saturated calomel electrode (SCE) were used as working, counter and reference, respectively. The dry sliding wear tests were done according ASTM G99 by the pin-on-disk method with the constant speed of 5cm/s, the sliding distance of 120m and the rotation radius of 5mm at room temperature. The 6mm alumina pin with the normal load of 5N in the test was used. The average of three tests was reported for each data.

### 3. Results and Discussion

#### 3.1. Monolayer coatings

In this study, some monolayer coatings were deposited for a better design of FG coatings using pulse parameters. For this purpose duty cycles of 45% and 80% were considered. The surface morphology and EDS of the above coatings are presented in Fig. 2. At the duty cycle of 45% the

amount of Cr deposition is very limited value and a Ni-rich coating was obtained. At the duty cycle of 80% the amount of co-deposited Cr is increased to about 83%. The previous studies have exhibited that Ni reduction follows a mass transfer control mechanism as the ratio Cr(III)/Ni(II) is very high in the electrodeposition bath [12]. Presence of off-time in the pulse plating provides an opportunity for Ni ions to diffuse to the surface of cathode [8]. The long off-time at the low duty cycle of 45% in comparison to 80% can compensate the depletion of Ni ions at cathode adjacent. In the other words, off-time diminishes the mass transfer mechanism. The reduction of Cr content at the low duty cycle can be explained by point view of current density. The average current density at the low duty cycle (considering a constant peak current density) is lower than this value at a high duty cycle. The high current density means a more negative potential that is desired for deposition of Cr rather than Ni. Furthermore, the deposition of Cr(III) occurs in two steps: (1) reduction of Cr(III) to Cr(II), (2) reduction of Cr(II) to Cr [13]. The second reaction

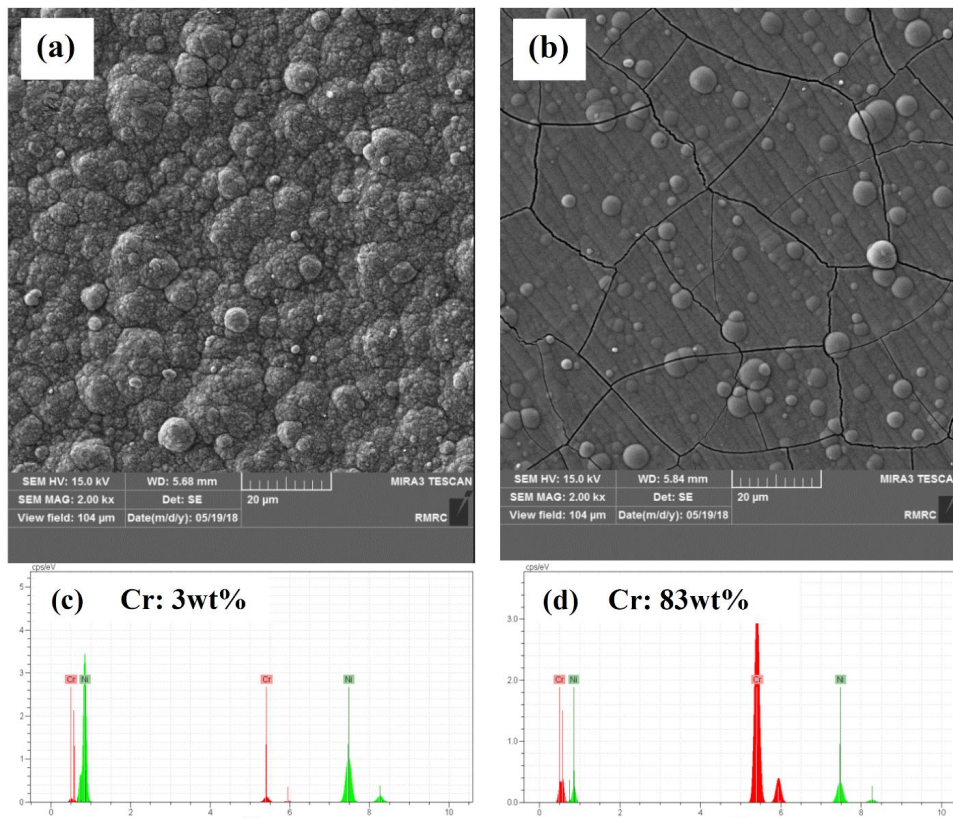


Fig. 2- The surface morphology and EDS pattern of monolayer Ni-Cr coatings deposited at frequency of 200Hz and duty cycle of (a)&(c) 45% and (b)&(d) 80%.

is rate determining stage for Cr deposition. As the accumulation of Cr(II) ions on the cathode occurs, the long off-time at low duty cycle provides a condition for moving away of Cr(II) ions. Then, the deposition of Cr is decreased [7].

The surface morphology of each specimen can be explained by Fig. 2. The morphology at the duty cycle of 45% is cauliflower-like and is nodular at 80% duty cycle. The cauliflower-like morphology is the character of Ni-rich coatings and the nodular-like is the morphology of Cr-rich ones that is presented in previous works [14]. As is obvious the density of cracks in Cr-rich coating is more than the one deposited at duty cycle of 45%. The cracks in the electrodeposited coatings are the direct result of decomposition of metallic hydrides and deposition stresses. The lower density of cracks at 45% can be attributed to the long off-time at a low duty cycle that provides the condition for hydrogen escape from cathode surface [15].

The effect of pulse frequency at constant duty cycle on the surface morphology and EDS results

are shown in Fig. 3. The frequency enhancement from 25Hz to 200Hz reduced the nodule size and the number of coarse nodules. The main effect of frequency is on the nucleation rate. Frequent disconnections at high frequencies lead to repeated interruption of ions reduction and frequent nucleation. The effect of frequency on the chemical composition of Ni-Cr isn't significant. This is similar to the previous researches that the chemical composition is independent of pulse frequency [16, 17].

### 3.2. Functionally graded coatings

The design of FG coatings was according to the investigations on the monolayer coatings. The pulse parameters were adjusted for deposition of Cr-rich layers on the top surface and the Ni-rich layer with less micro cracks adjacent to the substrate. The layer arrangement was shown in Fig. 1. The results of SEM investigation from cross section of FGD coatings are exhibited in Fig. 4. As the color difference of layers in BSE mode reveals, the bright layers near the substrate are rich of heavier metal

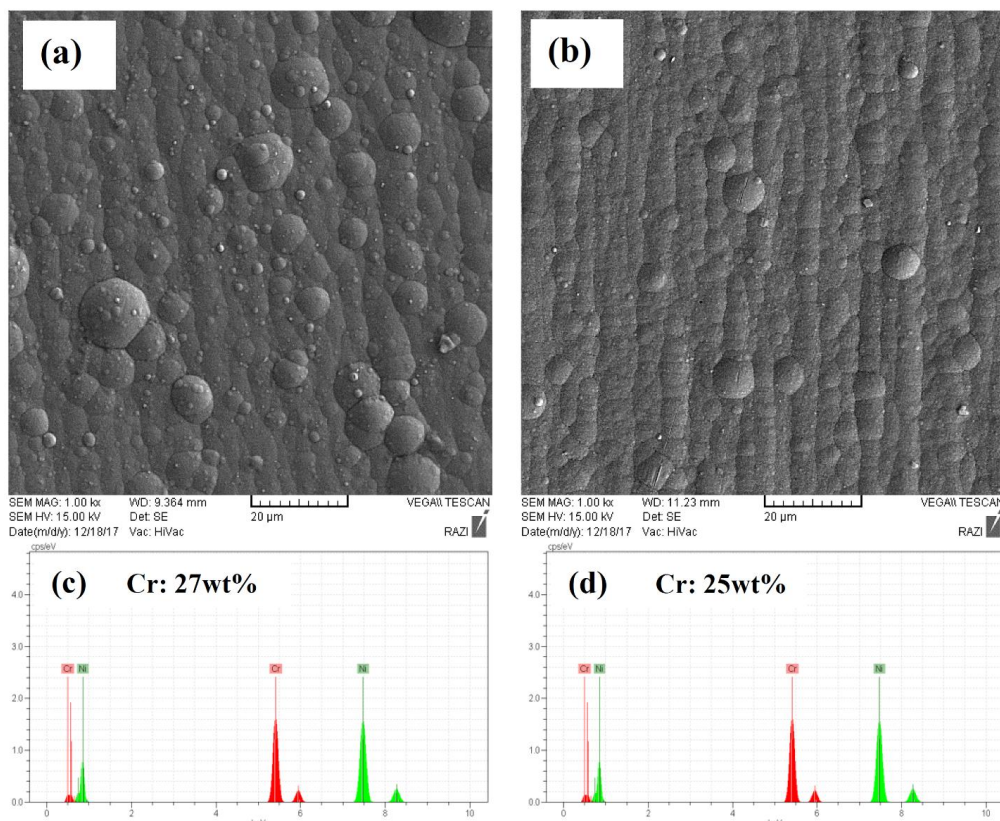


Fig. 3- The surface morphology and EDS result for monolayer coatings deposited at constant duty cycle of 60% and frequency of (a) & (c) 25Hz and (b) & (d) 200Hz.

(i.e. Ni) and the top layers are rich of lighter metal (i.e. Cr). The continuous alternation of the duty cycle in 7 steps from 45% to 80% caused a multilayer FG structure. In order to prove the above issue the EDS result of each sample is shown too. As observed the content of Cr from a minimum value for the first layer increases step by step to a maximum value for the top layer. The content of Cr in the FG

coatings for the layers deposited at the duty cycle of 45% and 80% is 3 and 83wt%, respectively, that is nearly same as those for monolayer ones. The other point from EDS results is that the pulse frequency has a negligible effect on the chemical composition of coatings, a result found also in several past studies [18]. The surface morphology of the above coatings is exhibited in Fig. 4 (e&f). The nodular-

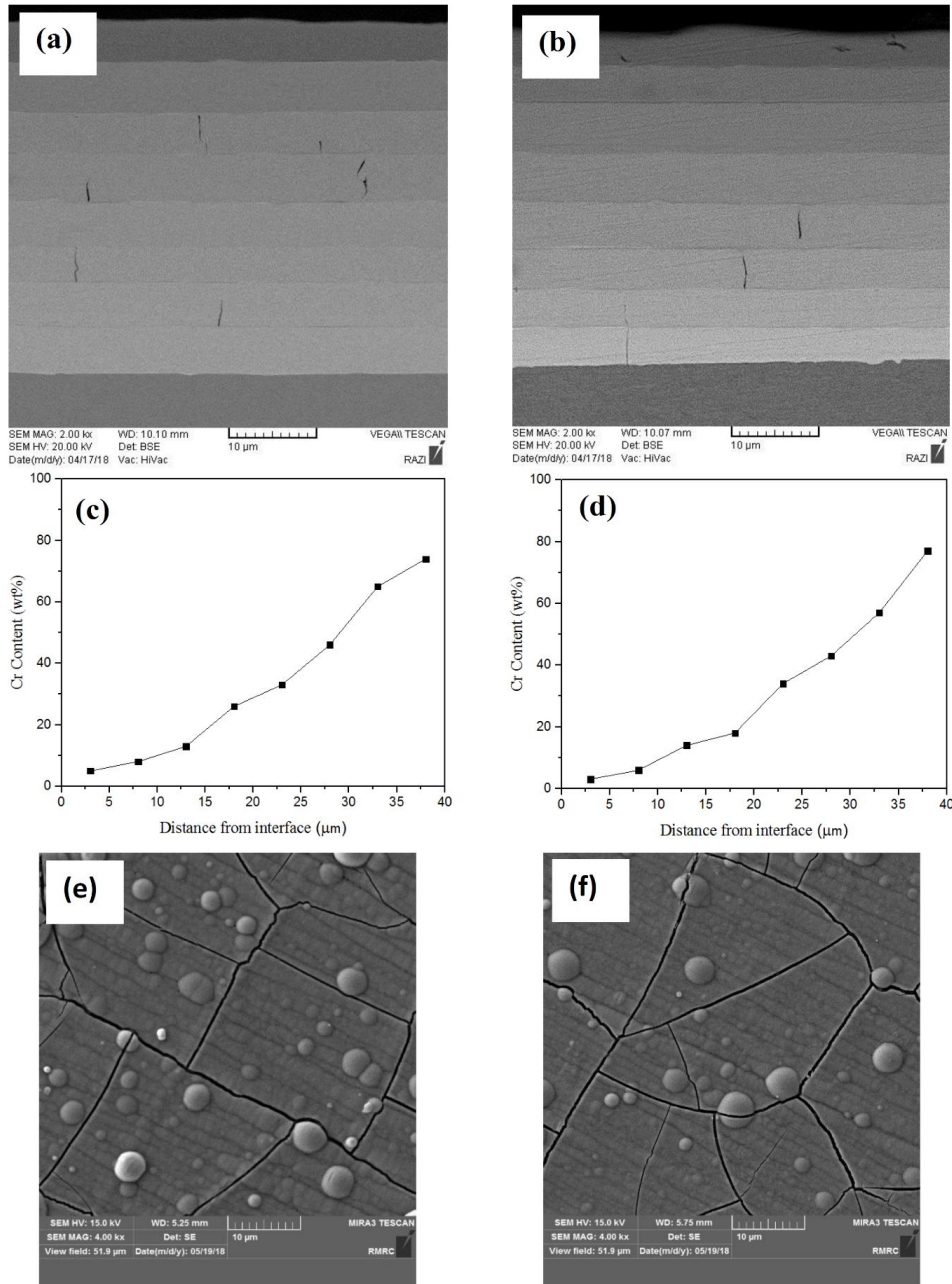


Fig. 4- The cross section view, corresponding EDS line and surface morphology of FGD coatings: (a), (c) and (e) FGD-25Hz and (b), (d) and (f) FGD-200Hz.

like morphology with many cracks on the top coat is the main features of these micrographs. As the top layer is electrodeposited at 80% duty cycle, the surface morphology of coatings is similar to the monolayer coating.

The results of SEM investigation on the FGF coatings are shown in Fig. 5. There is no change in

color contrast in cross section of coatings relying on the constant chemical composition or a slight change in chemical composition. The result of the EDS line confirmed this observation. The average content of alloying elements is nearly similar to the monolayer coatings. This result is same as the output of other researches that attempted to

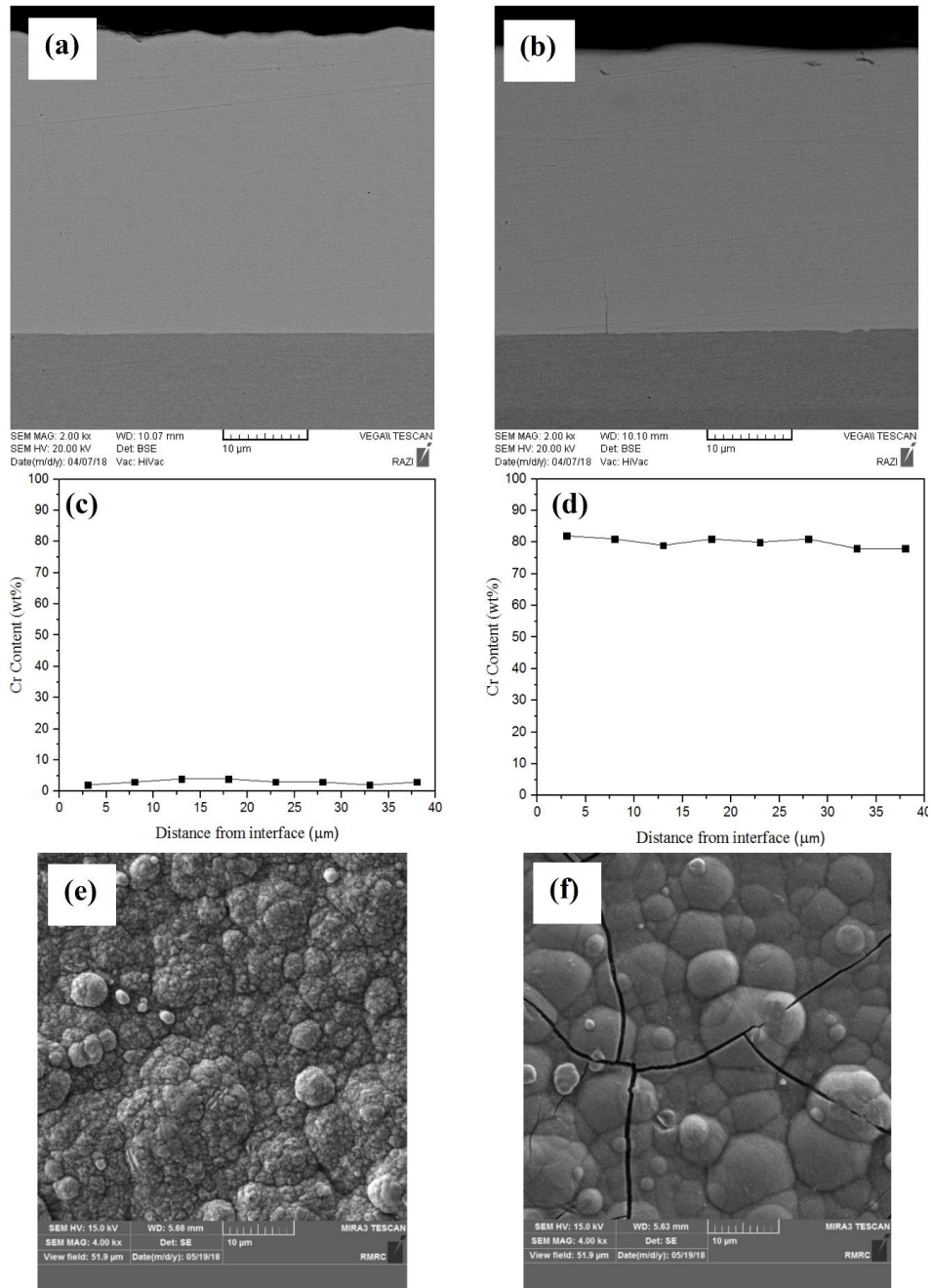


Fig. 5- The cross section view, corresponding EDS line and surface morphology of FGF coatings: (a), (c) and (e) FGF-45% and (b), (d) and (f) FGF-80%.

deposit multilayer coatings using the variation of pulse frequency. The morphology of these coatings is similar to the monolayer one and various changes of frequency have a slight change in the morphology and density of cracks.

### 3.3. Microhardness

It is expectable that the variation in chemical composition across the coating causes the variation in properties. The microhardness results for monolayer coatings are presented in Table 4. As is obvious the increasing of duty cycle increases hardness due to increase of Cr content and increasing frequency enhances the hardness due to grain refinement. The microhardness of different FG coatings is depicted in Fig. 6. In the case of FGD coatings, the hardness value increases gradually toward the surface. This is due to the increase of Cr content from first layers towards the outer layers. The Cr content can increase the

hardness of coatings[19]. In this graph increasing the frequency shifted the hardness value to higher values. This can be related to the grain refinement by frequency enhancement [20]. In the case of FGF coatings, the hardness value increases gradually from the first layer to the top surface. Although the hardness variation isn't sharp the effect of frequency variation can be observed via grain refinement.

### 3.4. Wear behavior

The pin-on-disk test was utilized for investigation of wear resistance of FG coatings. The specific wear rate of deposited coatings is presented in Fig. 7. The wear rate for FG coatings is decreased in comparison to the monolayer coatings. In order to explain the wear behavior two possible reasons should be considered; the microcracks and hardness. Although the hardness value for single layer coating deposited at 80% duty cycle is higher than the one deposited at 45% duty cycle,

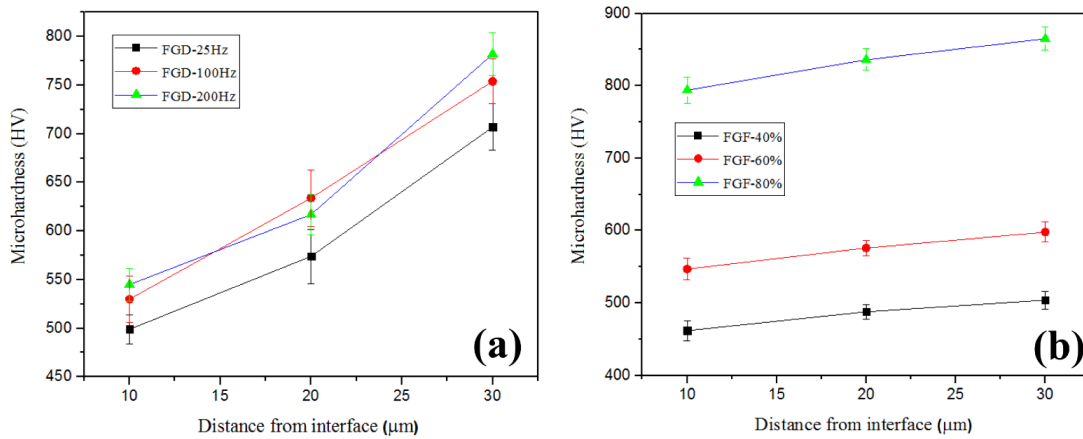


Fig. 6- The microhardness variation across the cross section of (a) FGD and (b) FGF coatings.

Table 4- The microhardness results for monolayer coatings

Duty cycle (%)	$i_p$ (Adm <sup>-2</sup> )	f (Hz)	t (min) for 15 µm
30	40	25, 100, 200	123
40	40	25, 100, 200	107
50	40	25, 100, 200	67.5
60	40	25, 100, 200	51
70	40	25, 100, 200	33
80	40	25, 100, 200	18

the density of microcracks is higher in the former one. Thus, the wear rate values are nearly similar. In the FGD coatings, the variation of chemical composition along the cross section has a beneficial effect that is explained in the previous section. In these coatings, the high hardness due to the layered structure [21], the decrease of microcracks and the increase of hardness towards the surface are responsible for better wear resistance compared with the monolayer coatings. For FGF coatings, the wear rate is decreased in comparison to the monolayer ones up to the 60% duty cycle. In fact, the high Cr content and in turn high hardness decreased the wear rate but at 80% duty cycle high microcracks density is detrimental for wear resistance. In the both FGD and FGF coatings the wear rate follows the Archard's theory [22] that is inversely proportional to the hardness values. The deviation of FGF-80% from above law is due to the

high density of microcracks in its structure.

In order to justify the wear rate results, the morphology of wear track was investigated using SEM micrographs. The wear tracks of FGD coatings are shown in Fig. 8. The abrasion mechanism as a dominant mechanism of wear is obvious in these coatings. Presence of microcracks in the wear track is the other feature in these coatings. The repeated rotation of alumina pin on the track can create and extend these cracks and finally, the joining of different cracks can separate a part of coating [22]. The microstructures relevant to the FGF coatings are presented in Fig. 9. The width of the track is representative of wear rate for each coating that is in good agreement with the results of Fig. 7. The main features of these micrographs are abrasion and plastic deformation. The SEM images of wear debris are exhibited in Fig. 10. The presence of plate-like debris is the conformance for the above

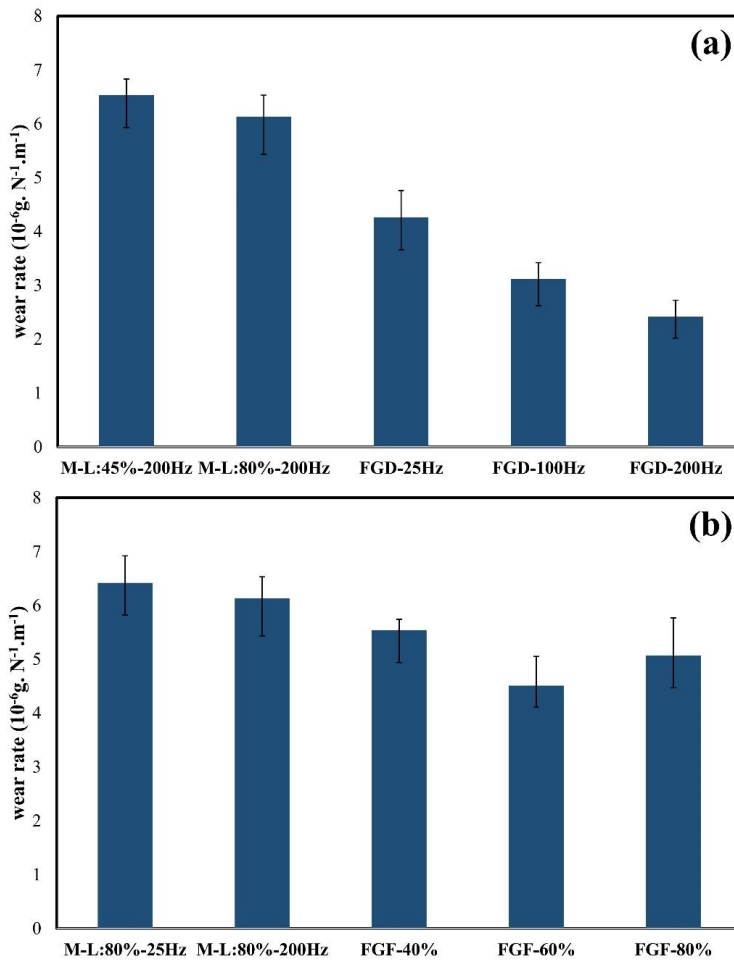


Fig. 7- The wear rate of (a) FGD and (b) FGF coatings in comparison to the monolayer coatings.

mechanism and chips like debris are the signs of abrasive wear [23].

The coefficient of friction (COF) for different coatings is shown in Fig. 11. As shown the COF decreases and then increases with increasing duty cycle. The factors affecting the COF and the tribological properties of the coatings are the microstructure and the chemical composition of the coating [24]. As previously stated, with increasing duty cycle, the chromium content of the coating is increased. One of the negative effects of the presence of chromium in the coating is the increase in the friction coefficient of the surface [25], which has shown itself to be in very high

levels of chromium (FGF-80% sample). This is, in fact, one of the major disadvantages encountered in hard chromium coatings. In many studies, high friction coefficients have been reported in the range of 0.6 to 0.8 for these coatings [25]. In the FGF coating, at 80% duty cycle with high chromium content, it is possible that, due to the microcracks of the coating, the ttf, the COF increases [19]. In the FGF-40% sample, because of its softness, it is likely that the because of plastic deformation in the coating a slightly higher COF than the optimum specimen was achieved. Regarding FGD coatings, it is seen that the COF curve is more uniform and more stable in terms of sliding distance than the

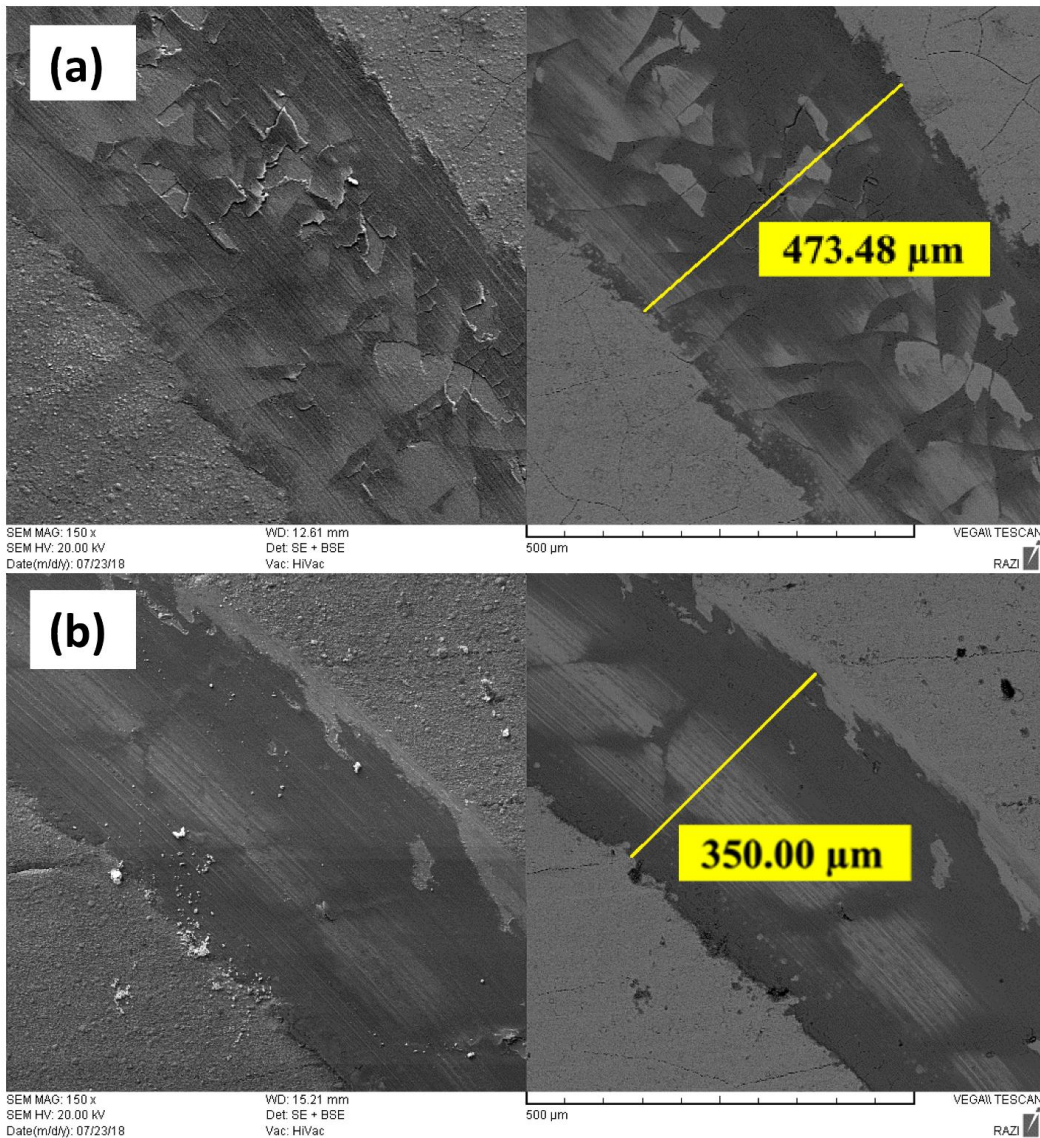


Fig. 8- The morphology of wear track of FGD coatings deposited at (a) 25Hz and (b) 200Hz frequency.

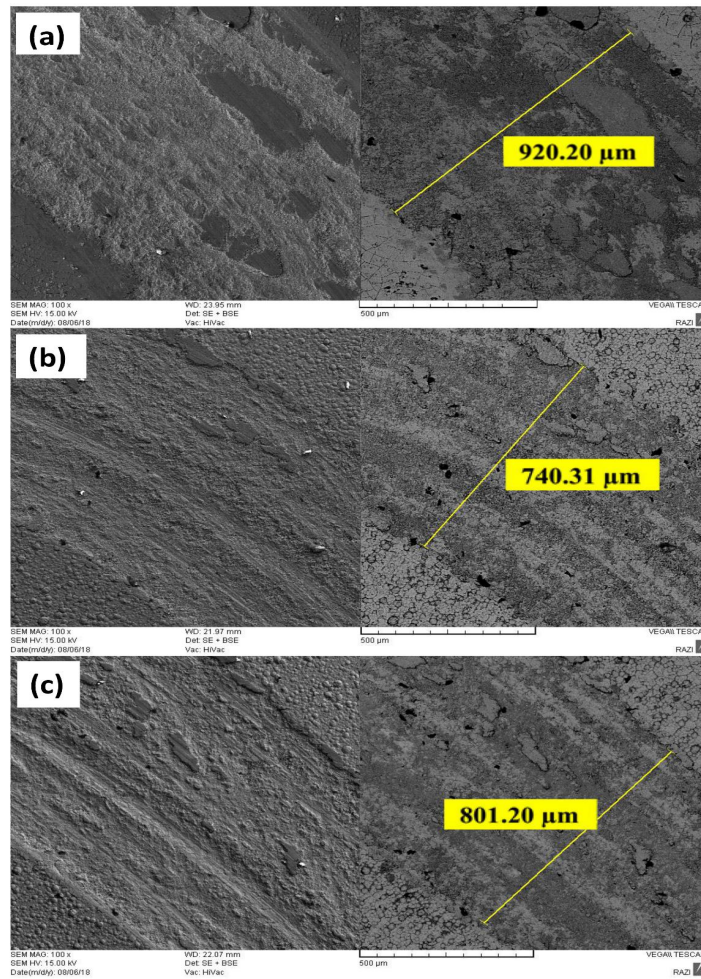


Fig. 9- The morphology of wear track of FGF coatings deposited at (a) 40% and (b) 60%, and (b) 80% duty cycle.

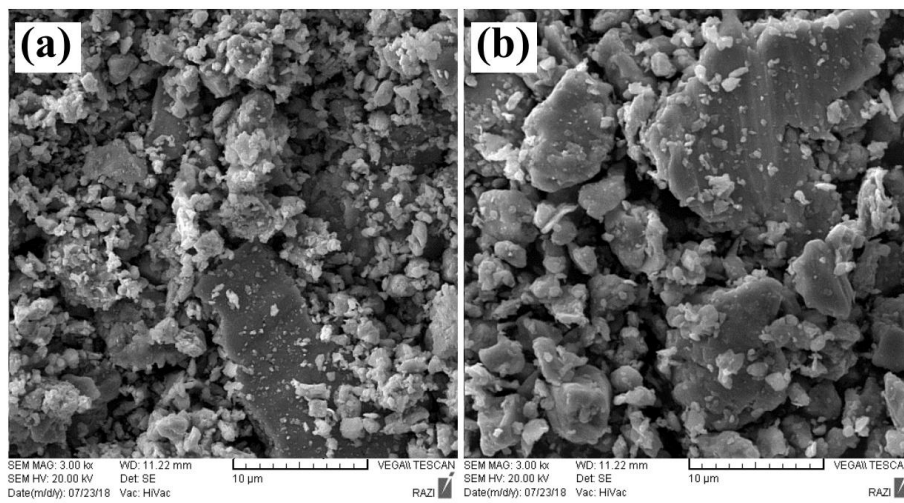


Fig. 10- The SEM micrograph of wear debris: (a) FGD-200Hz and (b) FGF-60%.

FGF coatings. This may be due to the formation of FG coatings as a result of a change in the chemical composition. In addition, in comparison to FGF coatings the COF in FGD coatings is lower, which is also attributed to the gradient nature of

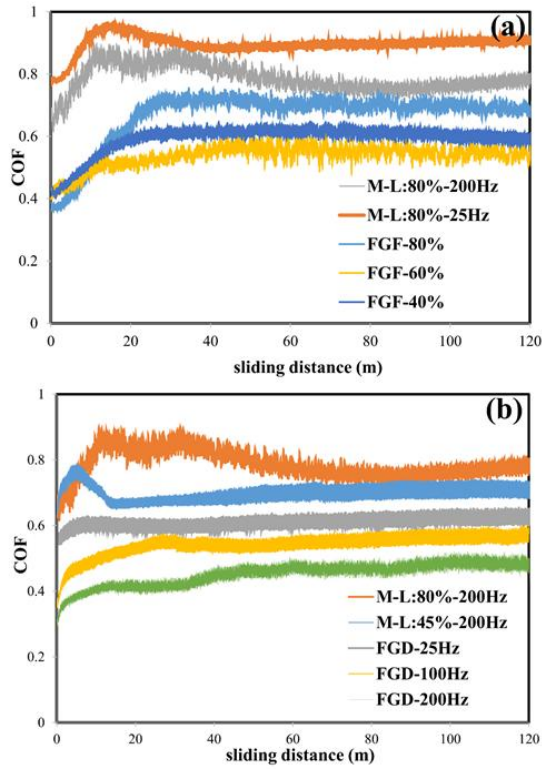


Fig. 11- The variation of COF versus sliding distance for (a) FGF and (b) FGD coatings.

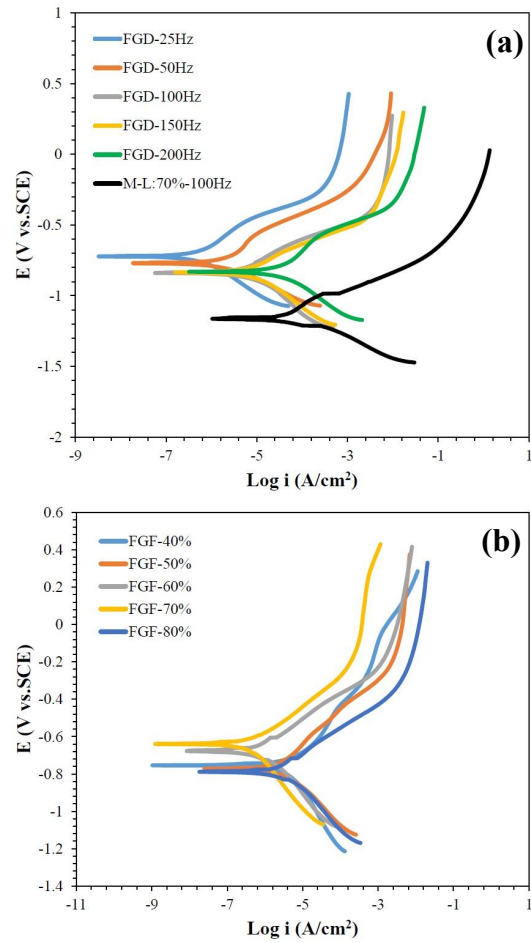


Fig. 12- The polarization plots of (a) FGD and (b) FGF coatings in comparison to the monolayer one.

Table 5- The extracted results of corrosion test for deposited FGD coatings

Duty cycle	$\beta_a$ (mV/decade)	$\beta_c$ (mV/decade)	$E_{corr}$ (mV vs. SCE)	$i_{corr}$ ( $\mu A/cm^2$ )
40 %	27	24	-537	16.3
50 %	26	32	-483	14.2
60 %	27	33	-451	13.7
70 %	21	31	-423	11.2
80 %	22	28	-707	21.5

Table 6- The extracted results of corrosion test for deposited FGF coatings

Duty cycle	$\beta_a$ (mV/decade)	$\beta_c$ (mV/decade)	$E_{corr}$ (mV vs. SCE)	$i_{corr}$ ( $\mu A/cm^2$ )
40 %	27	24	-537	16.3
50 %	26	32	-483	14.2
60 %	27	33	-451	13.7
70 %	21	31	-423	11.2
80 %	22	28	-707	21.5

the coating. In these coatings, the COF decreases with increasing frequency, so that the FGD sample deposited at 200Hz frequency has the lowest COF. As mentioned in the previous section, the grain size becomes finer with pulse frequency enhancement. Reduction of the COF with fine grain structure has been reported for Ni-Cu-W ( $\text{Al}_2\text{O}_3$ ) [26] and Ni-Zn- $\text{Al}_2\text{O}_3$  [27] gradient coatings.

### 3.5. Corrosion study

The polarization test for surveying corrosion resistance of electrodeposited coatings in 3.5% NaCl solution was considered. The polarization curves of FGD and FGF coatings are shown in Fig. 12. The corrosion current density ( $i_{\text{corr}}$ ) and corrosion potential ( $E_{\text{corr}}$ ) were derived from Tafel curves using linear extrapolation method and are shown in Table 5 and 6. The low  $i_{\text{corr}}$  and high  $E_{\text{corr}}$  are indications of better corrosion resistance. As presented, the  $i_{\text{corr}}$  increased and  $E_{\text{corr}}$  decreased with pulse frequency enhancement. Therefore, the pulse frequency has a negative effect on the corrosion resistance of FGD coatings. The main effect of frequency on the microstructure is grain refinement. It is reported in previous studies that the number (or density) of the active sites for corrosion and the diffusion routes for corrosive species in fine-grained materials is higher than in coarse-grained materials [28]. Hence, the finer grains at higher frequencies have a more active condition for corrosion. As observed in Fig. 12(b) the polarization curve for FGD coatings shifted to the up and left part of the plot comparing with the monolayer coating. As is explained in previous sections, the FGD coatings have several layers with a different chemical composition that have a distinct density of microcracks. These inhomogeneities and layer interfaces can deviate the path of corrosive species and a complex path may be created and in turn, the corrosion resistance enhances [29]. In the FGF coatings increasing of duty cycle improved the corrosion resistance up to 70% duty cycle and further increase to 80% decreased the corrosion resistance. This is due to the Cr content that is increased with duty cycle but the high density of microcracks at 80% duty cycle reduced the corrosion resistance [19].

### 4. Conclusions

In this research monolayer and FG coatings of Ni-Cr were deposited using pulse electrodeposition. In order to deposit FG coatings, two strategies were

employed. The first was the gradual increase of duty cycle (FGD coatings) and the second was the gradual increase of pulse frequency (FGF coatings). The main results of the research are as followings:

- The Cr content in the monolayer coatings is 83 and 3 wt% for 80 and 45% duty cycles and is nearly independent of pulse frequency.
- The continuous increase of duty cycle results in FG coatings that the Cr content increases in 7 steps from 3 to 83wt%. The continuous changing of pulse frequency has a slight effect on the chemical composition.
- The microhardness of FGD coatings on the top surface is in the range of 650-800  $\text{HV}_{0.01}$  that is decreased towards the interface. The high Cr content in the top layers is responsible for higher hardness.
- The wear rate of FGD coatings is lower than FGF and monolayer coatings due to the layered structure of coatings. The increase of pulse frequency reduces the wear rate that is attributed to the grain refinement as a result of high nucleation rate at higher frequencies.
- The wear mechanism of FGF and FGD coatings is recognized as abrasion and plastic deformation, respectively.
- Although the high density of microcracks at high Cr content results in the high COF and wear rate, the low COF for FGD coatings is because of the gradient nature of the coatings.
- The corrosion resistance of FGD coatings is higher than the FGF and monolayer coatings. This improvement is related to the layered structure of FGD coatings that may deviate the diffusion route of corrosive species. The higher pulse frequencies have a negative effect on the corrosion resistance due to the grain refinement.

### References

1. Mahdavi S, Allahkaram SR. Composition, characteristics and tribological behavior of Cr, Co-Cr and Co-Cr/TiO 2 nano-composite coatings electrodeposited from trivalent chromium based baths. *Journal of Alloys and Compounds*. 2015;635:150-7.
2. Bikulčius G, Češūnienė A, Matijošius T, Selskienė A. Dry sliding tribological behaviour of bilayer Cr/Cr coatings obtained in sulphate Cr(III) baths. *Transactions of the IMF*. 2018;96(3):130-6.
3. Li J, Li Y, Tian X, Zou L, Zhao X, Wang S, et al. The Hardness and Corrosion Properties of Trivalent Chromium Hard Chromium. *Materials Sciences and Applications*. 2017;08(13):1014-26.
4. Allahyarzadeh MH, Aliofkhaezai M, Rouhaghdam AS, Torabinejad V, Alimadadi H, Ashrafi A. Electrodeposition mechanism and corrosion behavior of multilayer nanocrystalline nickel-tungsten alloy. *Electrochimica Acta*. 2017;258:883-99.
5. Etmianfar MR, Heydarzadeh Sohi M. Corrosion resistance of multilayer coatings of nanolayered Cr/Ni electrodeposited

- from Cr(III)-Ni(II) bath. *Thin Solid Films*. 2012;520(16):5322-7.
6. Huang CA, Chen CY, Mayer J, Weirich T, Iskandar R. Nanosegregation of ternary Cr-Ni-Fe alloy deposits electrodeposited from a Cr<sup>3+</sup>-based bath. *Materials Letters*. 2013;93:107-10.
  7. Torabinejad V, Aliofkhaezrai M, Sabour Rouhaghdam A, Allahyarzadeh MH. Corrosion properties of Ni-Fe-Cr (III) multilayer coating synthesized via pulse duty cycle variation. *Materials and Corrosion*. 2016;68(3):347-54.
  8. Torabinejad V, Aliofkhaezrai M, Sabour Rouhaghdam A, Allahyarzadeh MH. Functionally Graded Coating of Ni-Fe Fabricated by Pulse Electrodeposition. *Journal of Materials Engineering and Performance*. 2016;25(12):5494-501.
  9. Torabinejad V, Aliofkhaezrai M, Sabour Rouhaghdam A, Allahyarzadeh MH. Tribological Behavior of Electrodeposited Ni-Fe Multilayer Coating. *Tribology Transactions*. 2016;60(5):923-31.
  10. Allahyarzadeh M, Aliofkhaezrai M, Rouhaghdam AS, Torabinejad V. Electrodeposition of multilayer Ni-W and Ni-W-alumina nanocomposite coatings. *Surface Engineering*. 2017;33(5):327-36.
  11. Torabinejad V, Rouhaghdam AS, Aliofkhaezrai M, Allahyarzadeh MH. Electrodeposition of Ni-Fe and Ni-Fe-(nano Al<sub>2</sub>O<sub>3</sub>) multilayer coatings. *Journal of Alloys and Compounds*. 2016;657:526-36.
  12. Adelhkhani H, Arshadi MR. Properties of Fe-Ni-Cr alloy coatings by using direct and pulse current electrodeposition. *Journal of Alloys and Compounds*. 2009;476(1-2):234-7.
  13. Harris TM. The Electrodeposition of Ni-Fe-Cr Alloys for Magnetic Thin Film Applications. *Journal of The Electrochemical Society*. 1995;142(4):1031.
  14. Lajevardi SA, Shahrabi T, Szpunar JA. Synthesis of functionally graded nano Al<sub>2</sub>O<sub>3</sub>-Ni composite coating by pulse electrodeposition. *Applied Surface Science*. 2013;279:180-8.
  15. Sharma A, Bhattacharya S, Das S, Das K. Fabrication of Sn nanostructures by template assisted pulse electrodeposition. *Surface Engineering*. 2016;32(5):378-84.
  16. Yang Y, Cheng YF. Fabrication of Ni-Co-SiC composite coatings by pulse electrodeposition — Effects of duty cycle and pulse frequency. *Surface and Coatings Technology*. 2013;216:282-8.
  17. Chen L, Wang L, Zeng Z, Xu T. Influence of pulse frequency on the microstructure and wear resistance of electrodeposited Ni-Al<sub>2</sub>O<sub>3</sub> composite coatings. *Surface and Coatings Technology*. 2006;201(3-4):599-605.
  18. Allahyarzadeh MH, Aliofkhaezrai M, Rezvanian AR, Torabinejad V, Sabour Rouhaghdam AR. Ni-W electrodeposited coatings: Characterization, properties and applications. *Surface and Coatings Technology*. 2016;307:978-1010.
  19. Sheibani Aghdam A, Allahkaram SR, Mahdavi S. Corrosion and tribological behavior of Ni-Cr alloy coatings electrodeposited on low carbon steel in Cr (III)-Ni (II) bath. *Surface and Coatings Technology*. 2015;281:144-9.
  20. Khorashadizade F, Saghafian H, Rastegari S. Effect of electrodeposition parameters on the microstructure and properties of Cu-TiO<sub>2</sub> nanocomposite coating. *Journal of Alloys and Compounds*. 2019;770:98-107.
  21. Kurmanaeva L, McCrea J, Jian J, Fiebig J, Wang H, Mukherjee AK, et al. Influence of layer thickness on mechanical properties of multilayered NiFe samples processed by electrodeposition. *Materials & Design*. 2016;90:389-95.
  22. Torabinejad V, Aliofkhaezrai M, Rouhaghdam AS, Allahyarzadeh MH. Tribological performance of Ni-Fe-Al<sub>2</sub>O<sub>3</sub> multilayer coatings deposited by pulse electrodeposition. *Wear*. 2017;380-381:115-25.
  23. Segu DZ, Choi JH, Yi S, Kim SS. Dry Sliding Tribological Properties of Fe-Based Bulk Metallic Glass. *Tribology Letters*. 2012;47(1):131-8.
  24. Das S, Banthia S, Patra A, Sengupta S, Singh SB. Novel bilayer Zn Ni/Ni Co SiC nanocomposite coating with exceptional corrosion and wear properties by pulse electrodeposition. *Journal of Alloys and Compounds*. 2018;738:394-404.
  25. Ma C. Electrodeposited nanocrystalline Ni-Co and Co-Ni-P coatings for hard chromium replacement (Doctoral dissertation, University of Southampton).
  26. Allahyarzadeh MH, Aliofkhaezrai M, Rouhaghdam ARS, Torabinejad V. Gradient electrodeposition of Ni-Cu-W(alumina) nanocomposite coating. *Materials & Design*. 2016;107:74-81.
  27. Shourgeshty M, Aliofkhaezrai M, Karimzadeh A. Study on functionally graded Zn-Ni-Al<sub>2</sub>O<sub>3</sub> coatings fabricated by pulse-electrodeposition. *Surface Engineering*. 2018;35(2):167-76.
  28. Ovid'ko IA. Deformation and Diffusion Modes in Nanocrystalline Materials. *International Materials Reviews*. 2005;50(2):65-82.
  29. Flores M, Muhl S, Andrade E. The relation between the plasma characteristic and the corrosion properties of TiN/Ti multilayers deposited by unbalanced magnetron sputtering. *Thin Solid Films*. 2003;433(1-2):217-23.